Vol. 04, Iss. 2 (2026) 271-286, DOI: 10.61552/JME.2026.02.011

JME

Journal of Materials and Engineering

www.jme.aspur.rs

Research article

Processing and Mechanical Characterization of Recycled PET-Sand-Chamotte Composite Roofing Tiles

Pierre Odi Nkoulou[a], Nguo Sylvestre Kanouo[a]*, Yannick Langollo Tchedele[b]

[a]*Department of Mining Engineering and Mineral Processing, National Advanced School of Mines and Petroleum Industries, University of Maroua, P. O. Box. 08 Kaélé, Far North, Cameroon.*
[b]*Local Materials Promotion Authority (MIPROMALO), P.O. Box, 2396 Yaoundé, Cameroon.*

Keywords:

Recycled PET
Chamotte
River sand
Ceramic–polymer composites
Roofing tiles
Mechanical properties
Sustainable construction materials

* Corresponding author:

Nguo Sylvestre Kanouo
E-mail: sylvestrekanouo@yahoo.fr

Received: 3 March 2026
Revised: 17 April 2026
Accepted: 3 May 2026

A B S T R A C T

This study determines the grain size distribution parameters (GSDP), specific gravity (SG), apparent density (AD), and major oxide composition of Monatélé-Sanaga river sand (MSRS) and chamotte; combined with recycled PET plastic wastes to process composite-polymer roofing tile's test specimens; on which physical and mechanical tests were performed to evaluate their quality. The aim of this study is to develop a sustainable construction material with a reduced environmental footprint. The GSDP(FM: 2.94, Cu: 3.6 , and Cc: 1.36), SG (2.59 g/cm³), and AD (1.5976 g/cm³) for MSRS show that it is medium to a bit coarse-grained with high variability, not well sorted, and with slightly low-density suitable for its use to produce polymer-composite roofing tiles. The sand is dominantly composed of SiO_2(65.79 wt.%) with significant Al_2O_3 (12.08 wt.%), K_2O (4.1 wt.%), and CaO (1.3 wt.%); probably due to the presence of quartz and aluminosilicate minerals important for the production of ceramic roofing tiles. Particle size (45.6 % of fine-grained size, 37.6 % of medium grained size, and 16.8 % coarse-grained size), SG (1.74 g/cm³), and AD (1.26 g/cm³) for chamotte classify it as fine to coarse-grained, very low-SG; and as lightweight insulating type (compatible with those used in processing composite roofing tiles). The chamotte (classified as low Al_2O_3 and slightly high alkaline type), is dominantly made up of SiO_2 (64.94 wt.%) with interesting Al_2O_3 (12.7 wt.%), CaO (1.03 wt.%), and K_2O+ Na_2O (6.49 wt.%), The AD (2.118-1.637 g/cm³), Wab (≤1.362 %) and P(≤ 2.032 %) place the formulated test specimens within the low water absorption, and less porous type. The FS (1.22- 6.12 MPa) and CS (9.76 -19.84 MPa) show an increase in the CS (much higher than that of standard ceramic roofing tiles).

1. INTRODUCTION

A roofing tiles is a manufactured, aesthetic, resistant, and durable building material designed to cover roofs from rain, snow, wind, sun, and other natural disasters [1-3]. It is dominantly processed by a thermal transformation of clay-rock to form ceramic roofing tile; with clay-rock being the main raw or the only material [4]. Alternative raw materials (e.g., tire powder; sand, metal, tile waste, rice husk ash, sugar can fiber, glass fiber, coir fiber, copper slag; gravel, granite dust, bamboo fiber, coal fly ash, and plastic) have been experimented in roofing tile's production [2, 4-13]. The diversity of roofing tile's raw materials leads to the distinction of many types of roofing tiles including: geopolymer roof tiles, metal roofing tiles, polymer roofing tiles, micro-concrete roofing tiles, concrete roofing tiles, and composite roofing tiles [1-3, 13]; with many factors governing their production. The key factors in roofing tiles production are: (1) the availability and characteristics of raw materials; (2) the processing techniques; (3) the cost encountered during the production of the tiles; and (4) the quality and marketing of the produced tiles [2,4]. Because of the lack of raw material in some localities, the high cost of production of traditional ceramic roofing tiles, environmental (e.g., deforestation, and waste dumping) and health problems (e.g., air-water pollution) generated during their production [4 8], research are now focused on how to produce low-cost and health-environmental-friendly roofing tiles with local adapted and available raw materials. Polymer-sand roofing tiles in particular, produced by thermal combination of sand and polymer (e.g. plastic, nylon, or teflon), are light weight, stiff, less prone to salt and chemical attacks, and have good insulation properties [3]. Their production stands as part of solution to global plastic management. Polymer-ceramic composites incorporating recycled plastics and local aggregates represent a promising route toward sustainable construction materials with reduced environmental footprint [14].

Plastics (long chains monomers: polymers), are not environmental-friendly products; as they are not fast-biodegradable; causing environmental pollution (e.g., landfilling), and health problems in human and other organisms [15-17]. Their long-time breakdown frees dangerous pollutants (e.g., furans, dioxins, Bisphenol-A, thalates, antiminitroxide, brominated flame retardants, and poly-fluorinated chemicals) harmful to human, animals, and environment [15, 17, 18]. Cameroon, like many countries in the world produces and uses plastics. Part of plastics used in Cameroon is imported as market products or goods packaging envelops and bags from neighboring Nigeria, Equatorial Guinee, Tchad, and Central African Republic; but also, from Asia, Europe, America, and Canada; which therefore, increase the rate of waste plastic pollution. Proportionally, Low Density Polyethylene (LDPE) is the most produced plastic waste (35 %), followed by Polyethylene Terephthalate (PET: 31 %), High Density Polyethylene (HDPE: 10%), and PVC and polyisoprenes (8 %) [11]. Plastic wastes are not industrially managed in Cameroon [11]. Minor quantity is recycled by smaller units found mainly in Douala and Yaoundé. Most plastic wastes are dumped open air in the greater part of the country; causing landfilling, soil pollution, water (stream, river, and ocean) pollution with direct impact biodiversity. Experimental works (example of that of Nkotto et al., [11]) have being carried out on how to recycle plastic waste in plastic--river sand-based composite roofing tiles production, in which PET plastic constitute the binder. Much still has to be done to recycle plastic waste in Cameroon, in order to minimize negative environmental and health impact of this material. The current research is part on the solution to try to minimize environmental and health impact of plastic wastes by recycling them in an experimental production of river sand-chamotte-plastic waste composite roofing tiles.

In general, to produce roofing tiles, adapted raw materials should be available in an industrial quantity (for an industrial production). These raw materials are characterized in order to see if they meet the standard requirements; and if possible, verify if their exploitation and processing will not cause significant environmental and health problems. The characterization of raw materials used to process roofing tiles depends on their nature. For examples, geochemical, geotechnical, physical, and mineralogical characterizations are carried out on clays and sand [2, 8, 11]. Geochemical and mineralogical analyses are carried out on fly ash and tile waste [8]. Processed tiles are also characterized to verify if they meet the required

standards. Compression strength test, tensile strength test, flexural strength test, bulk density test, water absorption test, porosity test, thickness swelling test, thermal conductivity and thermal resistance test, microstructural test, moisture content test, firing shrinkage test, and/or wear test are often carried out (e.g., [7, 8, 11-13]).

In his study, raw materials (Monatélé-Sanaga river sand and chamotte) are physically and geochemically characterized, before their thermal combination with PET plastic to produce sand-chamotte-PET plastic-based composite polymer roofing tile's test specimens. Processed tile's test specimens are physically and mechanically characterized in order to verify if they meet the required standards. Specimens with standard requirement are used to process the river sand-chamotte-PET plastic-based composite tile's prototypes.

2. MATERIALS AND METHODS

This part presents materials and methods used for collection of the raw materials (river sand: Figure 1, chamotte: Figure 2, and plastic bottles: Figure 3), and to characterize the sand and chamotte. Are also presented, materials and methods used to process the sand-chamotte-plastic composite-roofing tile's test specimens, and to carry out quality tests on processed tile's specimens.

Fig. 1. Sampling of Monatélé-Sanaga river sand

2.1 Sampling of raw materials

Fresh river sand sample was collected in River Sanaga at Monatélé (Figure 1). A sand sampling specialist went into the river with a 10 liters plastic bucket to collect the sample, many times to obtain a total of 200 kg. The collected sample was packaged in polystyrene bags. Chamotte sample (200 kg) was sampled at the Local Materials Promotion Authority (MIPROMALO). Plastic bottles were collected in the town of Yaoundé in different waste dump. Only polyethylene terephthalates (PETE or PET) type plastics were collected and packaged (Figure 3).

Fig. 2. Oven-drying of chamotte.

Fig. 3. Sampled of PET plastic wastes.

2.2 Characterization of Monatélé -Sanaga river and chamotte

The characterization of Monatélé-Sanaga river sand and chamotte includes the grain size distribution analyses, the specific gravity test, and the determination of the apparent density. They were carried in laboratories at the Local Materials Promotion Authority (MIPROMALO) in Yaoundé (Cameroon). The major oxides geochemical analysis carried on the two raw materials mentioned, was done at the geochemical laboratory in CIMENCAM Figuil, North Region, Cameroon.

The grain size distribution analysis was performed by dry sieving for particles greater than 80 µm and by sedimentation for particles lower than 80 µm. These particle size distribution analyses were carried out according to the NFP94-057 [19] standard. For dry sieving, 500 g of each sample was oven-dried at 105 °C for 24 h, put, and sieved in column of eight sieves (with a mesh of 4 mm, 2 mm, 1 mm, 0.8 mm, 0.5 mm, 0.2 mm, 0.1 mm and 0.08 mm, respectively), placed on an electro-vibrating machine. Each retained fraction was sampled, weighed, and the obtained value used to calculate the percentage retained material for each sieve via the formula (1)

$$\%Rf = \frac{Wr}{Tw} \times 100 \quad (1)$$

With: Wr: Weight of retained material of each sieve (g); Tw: Total weight of retained material for all sieves(g); %Rf: Percentage of retained material for each sieve (%).

The obtained percentage of retained material for each sieve was added together to obtain the cumulative percentage of retains (CPR). The cumulative percentage of passing-by was calculated via the formula (2) and used to construct the particle size distribution curve.

$$CPP = 100 - CPR \quad (2)$$

With CPR: Cumulative percentage of retained material (%); CPP: Percentage of passing material (%).

The obtained results were used to determine the fineness module (FM), coefficient of uniformity (Cu) and curvature coefficient (Cc). The FM was calculated according EN12620 [20] standard with formula (3). The uniformity coefficient and curvature coefficient (were calculated via formula (4) and (5), respectively.

$$FM = \frac{1}{100}\sum cumulative\ percentage\ of\ sieved\ retains\ (0.125 - 0.25 - 0.50 - 1 - 2 - 4) \quad (3)$$

$$Cu = \frac{D_{60}}{D_{30}} \quad (4)$$

$$Cc = \frac{(D_{30})^2}{D_{10} \times D_{60}} \quad (5)$$

With D_{60}: diameter of the particles which corresponds to 60 percent of the passers-by, D_{30}: diameter of the particles which corresponds to 30 percent of the passers-by, D_{10}: diameter of the particles which corresponds to 10 percent of the passers-by.

For sedimentation particle analysis, fraction with grain size less than 80 µm was separated from suspension and oven-dried. This fraction was oven-dried at 105 °C for 24 h. 40 g of dried sample was mixed in a bottle, with 220 ml of distilled water; and 30 ml of a solution of sodium hexametaphosphate, closed and kept for 24 h. After 24 h, the bottle with the mixture was agitated, before pouring in a burette; and added 1000 ml of distilled water. A densimeter was immersed in the solution to measure the evolution of the density in 24 h, at the regulated time 30 s, 1 min, 2 min, 5 min, 10 min, 20 min, 40 min, 80 min, 4 h, and 24 h, respectively. The volume was calculated via formula (6).

$$v = \frac{(\gamma s - \gamma w)}{18\eta} D^2 \quad (6)$$

The specific gravity test was carried out according the EN1097-6 [21] standard. It was performed by Archimedes method using a measuring scale (Gibertini) with a sensitivity of ± 0.0001 g, and three pycnometers of different weight. Each pycnometer was weighed. 20 g of sample was put into each of pycnometer and weighed. Distilled water was added into pycnometer + sample up to the measuring line and weighed. The obtained weight values and that of pycnometer with water were used to calculate the specific weight via the formula (7).

$$SG = \frac{(M2 - M1)}{(M2 - M1) - (M3 - M4)} \quad (7)$$

With M1: Weight of an empty pycnometer (g); M2: Weight of the pycnometer with dried sample (g); M3: Weight of the pycnometer with dried sample and distilled water (g); M4: Weight of pycnometer with water (g); SG: Specific gravity of each sample (g/cm^3).

The apparent density of sample Monatélé-Sanaga river sand and grog were determined according the ASTMD2854 [22] standard. The procedure was as follows; each collected sample was crushed and put into a cylinder at a corresponding volume (V). The cylinder with sample was weighed and the corresponding weight (M) recorded. The corresponding weight and volume were used calculate the apparent density via formula (8).

$$AD = \frac{M}{V} \quad (8)$$

The geochemical analysis carried out with the aid of an XRF (German XRF9900 thermo spectrometer) (as described in Hamadou et al., [23]), include the determination of the proportion of loss of ignition (%LOI) and the proportion of element's oxides. The proportion of LOI was determined as follows; 1.0 g ± 0. 05 ± 0.000 5 g (mo) of each sample was put in an inflamed crucible for a total weight of m1. The sample with crucible were carried into an electric oven for calcination at regulated temperature of 1150 ± 25 °C at 20 min. After calcination, the calcined sample and crucible were removed and rapidly carried to the desiccator to cool at the room temperature. The calcined-cooled sample was removed, weighed and the corresponding weight (m2) recorded. The percentage of LOI (%LOI) was calculated via formula (9)

$$\%LOI = \frac{m1-m2}{m0} \times 100 \quad (9)$$

The element oxides composition of each of the sample was determined on prepared pearl. The procedure was as follows; 1.0 g ± 0.05 g of calcined sample and 8 g of tetraborate of lithium were put into a crucible, and homogenized. 1 ml of lithium bromide was added into the mixture with the aid of a micropipette, mixed, and put in an electrical furnace for melting by heating at 1150 ± 25 °C for 20 min. The hot melt was removed and poured into a mold to form a pearl after cooling. The obtained value of LOI was introduced of the XRF spectrometer after introducing the pearl. The sample's oxide composition (wt.%) appears during manipulation XRF spectrometer on the connected computer monitor.

2.3 Processing of the composite-roofing tiles

After the characterization of the raw materials, (Monatélé-Sanaga river sand and chamotte), the next step was sample preparation and formulation of test specimens. The sample preparation and formulation of test specimens were done at the Local Materials Promotion Authority (MIPROMALO) in Yaoundé (Cameroon). Sand samples and chamotte were oven-dried separately at 105 °C at 24 h. The dried sands were sieved with 2 mm mesh sieve; whereas, chamotte samples were crushed and sieved with a 250 µm mesh sieve. Plastic bottles were emptied, washed to remove all unneeded material, pieced, and sun-dried.

Fig. 4. Formulated river sand-chamotte-plastic composite roofing tile's test specimens (4 cm x 4 cm x16 cm) size.

Composite roofing tiles test specimens (Figure 4) were formulated with the proportion of material presented in Table 1. The percentage of used plastic is 30 % (T30F), 35 % (T35F), 40 % (T40F), 45 % (T45F), and 50 % (T50F). Chamotte was used to partially replace sand at 0 %C, 5 %C, 10 %C, 15 %C, 20 %C, and 25 %C for a total of % of plastic + % of sand+ % of chamotte = 100 %. A total of 60 test specimens were formulated as follows; weighed-pieced plastic bottles, were wood-fire fused in a pot at 170 to 260 °C (constantly monitored with a test 925 AG Germany thermocouple). The melted plastic was constantly mixed to homogenize. Weighed sand and chamotte were added to the melt and homogenized to obtaine a paste. The paste was poured into prepared molds (metal prismatic molds of 4x4x16 cm) soaked in motor oil and compacted in the molds to ensure uniformity before hardening. The mold was cooled open air before demolding.

Table 1. Proportion (%) of raw materials used to process roofing tile's test specimens (%S: Proportion of river sand; %C: Proportion chamotte).

Formulation with plastic proportion	Proportion of sand (S) and chamotte (C)					
	0 % C	5 %C	10 %C	15 %C	20 %C	25 %C
T30F	70 %S	65 % S	60 %S	55 %S	50 % S	45 %S
T35F	65 %S	60 % S	55 %S	50 %S	45 %S	40 %S
T40F	60 %S	55 %S	50 %S	45 %S	40 %S	35 %S
T45F	55 %S	50 %S	45 %S	40 %S	35 %S	30 %S
T50F	50 %S	45 %S	40 %S	35 %S	30 %S	25 %S

T30F :30 % of plastique, T35F ; 35 % of plastique, T40F ; 40 % of plastique, T45F ; 45 % of plastique, T50F ; 50 % of plastique

2.4 Quality tests carried out formulated specimens

Quality tests carried out formulated composite roofing tile's test specimens include the physical tests (determination of the apparent density, water absorption, and the porosity). They also include the mechanical tests (the determination of the flexural and compression strength). They were carried out on 60 formulated specimens (2 tests/formulation).

The apparent density was determined by immersing each specimen in water found in the pycnometer. The procedure was as follows; Each dried sample was weighed and the corresponding weight (Wd) recorded. The weighed specimen was immersed in water found in the pycnometer. The volume (Vd) of water displaced during the immersion of the specimen was measured. The obtained value and the weight (Wd) were used to calculate the apparent density via formula (10).

$$AD = \frac{Wd}{Vd} \quad (10)$$

With Wd: Weight of the dried specimen before immersion (g), Vd: Volume of water displaced during immersion (cm^3), AD: Apparent density (g/cm^3).

The water absorption test was carried according the ASTMC20 [24] standard. Each dried test specimen was weighed for a corresponding weight (wd). The weighed sample was immersed in water for 24 h. The immersed specimen was removed, wiped, and weighed. The obtained weight value wh and wd were used to calculate the water absorption via formula (11).

$$Wab = \frac{wh - wd}{wd} \times 100 \quad (11)$$

With wh: Weight of the humid specimen from immersion (g), wd: Weight of the dried specimen before immersion (g), Wab: Water absorption (%).

The porosity test was carried according the NFP18-459 [25] standard. Each dried specimen was weighed (wd). The dried specimen was immersed in water and removed after 24 hours. This sample was sponged and weighed. The obtained weight (wh) was recorded. The sponged specimen was weighed with scale hosting hydrostatic device; after being systematically immersed in water found in the weighing scale. The weight of water (w_w) was obtained and used to calculate the porosity via formula (12).

$$P = \frac{wh - wd}{wh - ww} \times 100 \quad (12)$$

With wh: Weight of the humid specimen from immersion (g), wd: Weight of the dried specimen before immersion (g), ww: Weight of water in the hydraulic device during the second immersion (g), P: Porosity (%).

The flexural and compression strength tests carried out on each test specimen, were done with the aid of a 500 KN hydraulic press machine (Ele International). These tests were carried out according the EN12390-2 [26] standard. The flexural strength test was carried out as follows; a load force was applied vertically on the opposite side face of each specimen placed horizontally on the plate of the hydraulic machine. This force was time-increased until failure. The corresponding force value was read directly on the used machine. This value was used to calculate the flexural strength, with this formula (13).

$$FS = \frac{3FL}{2bh^2} \quad (13)$$

With F: Applied load force (KN), L: Distance between two support points, b: Width of the specimen (mm), h: Thickness of the specimen (mm), FS: Flexural strength (MPa).

The compression strength test was carried out on specimens from the flexural strength test. A load force was applied on the 4 x 4 cm^2 surface of the specimen. This force was increased until failure. The corresponding force was read on the device. This force value and that of the surface were used to calculate the value of the compression strength with formula (14).

$$CS = \frac{F}{S} \quad (14)$$

With, F: Applied load force (KN), S: Surface area on which the load force was applied, CS: Compression strength (MPa).

3. RESULTS AND DISCUSSIONS

The obtained results for particles size analysis, specific gravity, apparent density and geochemical analysis for Monatélé-Sanaga river sand and used chamotte are presented and discussed separately, leading to their characterization as raw materials for the formulation of plastic recycled composite roofing tiles. Quality tests results from water absorption test, porosity test, apparent density test, flexural strength test, and compression test carried out on formulated tile's test specimens are also presented and discussed.

3.1 Characteristics of Monatélé-Sanaga river sand and chamotte

The particle size distribution plot diagram for Monatélé-Sanaga river sand and used chamotte are presented in Figure 5. Calculated parameters such as fineness modulus (FM), uniformity coefficient (Cu), and curvature coefficient (Cc) helped to characterize the sand sample (Table 2). The FM for the Monatélé-Sanaga river sand calculated based EN12620 [20] standard is 2.94; greater than that of river sand in Maroua with FM (≤ 2.91) studied by Nafissatou et al., [27]; and that of sand from river Sanaga (FM: 2.03) studied by Nkotto et al., [11] (see Table 2).

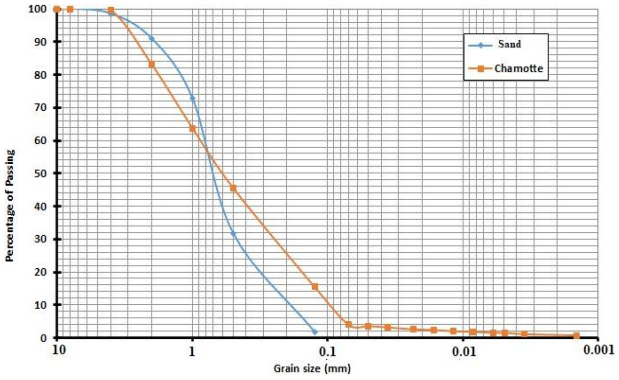

Fig. 5. The particle size distribution curves for the Monatélé-Sanaga river sand and used chamotte.

Table 2. Grain size distribution parameters, SG and AD for studied sand compared with those published for some river sands.

Sample	FM	Cu	Cc	SG (g/cm³)	AD (g/cm³)
Monatélé -Sanaga river sand	2.93	3.6	1.36	2.59	1.60
Maroua River sand [27]	2.43-2.91	2.36-3.37	0.4-0.99	-	1.44-1.54
Sanaga alluvial sand [11]	2.03	-	-	-	-
River sand in Opara et al., [31]	2.54	2.11	0.9	2.64	1.570
River sand in Abdias et al., [32]	-	-	-	2.5-2.7	1.6-18
Acceptance limit for concrete in Opara et al., [31]	2.2-3.2	-	-	2.6-2.8	

FM is usually used to classify sand samples [28, 29]. When FM of a sand sample is within 1.8 to 2.2, the analyzed sample is fine-grained; when FM is within 2.2 to 2.8, the sand sample is preferential; it is a bit coarse-grained, when FM is within 2.8 to 3.3 [28]. According to the ASTM C33 [29] standard, when the FM is within 2.5 to 3.5, the studied sand is classified as medium-grained. The FM (2.94) for the studied sand sample is within 2.8 and 3.3; which belongs to a bit coarse-grained class in Ghomari and Bendi-Ouis [28] classification scheme; but, fall within medium-grained sand in ASTMC33 [29] standard classification. This sand sample is lightly to be medium to a bit coarse-grained, slightly different to medium grained from Maroua [27]; and completely different to predominantly fine-grained sand from river Sanaga [11]. In Ghomari and Bendi-Ouis [28] a bit coarse-grained class sands formulate resistance concretes with limited segregation effect. This shows that the studied sand can be used to formulate resistance concretes with limited segregation effect. Nkotto et al., [11] used their sand sample to experimentally process plastic-based tiles. They realized that formulations with 20 % of plastics have lower water absorption in line with the ISO62 [30] standard for roofing tiles. From this difference, it is not possible to draw a conclusion at this stage. This conclusion would be done after quality tests on formulated tile's test specimens.

The obtained value of the coefficient uniformity (Cu) is 3.6; and that of Coefficient of curvature (Cc) is 1.36 (Table 2). The obtained Cu is higher that of river sand (Cu: 2.11) presented in Opara et al., [31] and that of river sand in Maroua (Cu 2.36 to ≤ 3.37) studied by Nafissatou et al., [27],

but, greater 3 which for Abdias et al. [32] shows that the particle size is uniform or even tight. The Cc (1.36) is higher than that of river sand (Cc= 0.96) presented in Opara et al., [31] and that of river sand in Maroua (Cc: 0.44 to < 1, classified as poorly graded; [27]); but, within the range limit (Cc: 1 to 3) for well graded soil, as classified in Abdias et al., [32]. The studied sand sample with its Cc slightly higher than 1, seems to be well graded.

Particle size analysis carried out on crushed chamotte, shows that it is made up of 45.6 % of fine-grained particles, 37.6 % of medium-grained particles, and 16.8 % coarse-grained particles (Table 3). This shows the predominance fine-grained particles over medium and coarse-grained particles, respectively. The predominance of fine-grained particles over medium and coarse-grained particles was also obtained by Al-Taie and Abu-Hamatteh [33] after grain size distribution analysis of their chamotte. Slight differences are observed between the result in this study and those presented in Al-Taie and Abu-Hamatteh [33] (Table 3). These include the proportional difference, with values for the studied chamotte being lower than those of Al-Taie and Abu-Hamatteh [33]; excepting that of the medium-grained fraction. The characterized chamotte can be named fine to coarse-grained type; which might be a good parameter for its use in processing sand-chamotte-plastic composite roofing tiles.

Table 3. Particle size, SG and AD for used chamotte compared with those published by other authors.

Sample	Grain size proportion			SG (g/cm^3)	AD (g/cm^3)
	Fine grained size (%)	Medium grained size (%)	Coarse grained size (%)		
Chamotte (this study)	45.6	35.6	16.8	1.74	1.26
Chamotte in [33]	50	20	30	-	-
Chamotte in [34]	-	-	-	2.74	1.43

The specific gravity (SG) for Monatélé-Sanaga river sand sample is 2.60 g/cm^3(Table 2). This value falls within those of river (2.5-2.7 g/cm^3) in Abdias et al., [32]; but, slightly below that of river sand (2.64) presented in Opara et al., [31]. For Opara et al., [31] the acceptance SG limit values for river sand used in concrete production range from 2.6-2.8 g/cm^3. The SG value for the studied river sand is very close the minimum limit SG (2.6 g/cm^3) accepted for concrete production; which shows that the Monatélé-Sanaga river sand is good in concrete production.

The specific gravity for chamotte is 1.74 g/cm^3 (Table 3). This value is out of the SG typically range limit (2.6-3.0 g/cm^3) for chamotte. It is also less than that of chamotte (2.741 g/cm^3) Soukup et al., [34] used to process geopolymer composites for energy storage. The cause of this relatively low SG is difficult to determine at this stage; although, many factors such as the nature of raw material used to process the chamotte and processing technic can influence its specific gravity [34]. This chamotte can be classified as very low-SG type; probably good for composite roofing tiles processing.

The apparent density of the rive sand sample is 1.598 g/cm^3 (Table 2). The apparent density for river sand ranges from 1.6 to 1.8 g/cm^3 [32]. The obtained density for Monatélé-Sanaga river sand is very close to the minimum value (1.6 g/cm^3) for river sand apparent density presented in Abdias et al., [32]. For Abdias et al., [32], poorly sorted sands with more porous minerals will have lower bulk densities, and coarse-grained, when the density is close 1.6 g/cm^3. If based on Abdias et al., [32] study, the Monatélé-Sanaga river is coarse-grained, and not well sorted. The obtained density is greater than that of river sand from Maroua (AD: 1.44 to 1.54) study by Nafissatou et al., [27]; but, slightly higher that of river sand (1.570 g/cm^3) studied by Opara et al., [31]. Nafissatou et al., [27], based on the NF P18-554 [35] standard, classified their Maroua river sand as slightly low-density sand. The studied sand with its apparent density very close to the minima value (1.6 g/cm^3) required for river sand, and higher than those Maroua river sand and that of Opara et al. [31] can be considered slightly low-density sand; probably good for composite roofing tiles processing.

The obtained apparent density for chamotte used to formulate the sand-chamotte-plastic-based composite tiles is 1.26 g/cm^3(Table 3). The

apparent density has been used to classify chamotte in two main groups [34]: (1) lightweight insulating types with the values of apparent density ranging from 0.3 to 1.3 g/cm^3; and (2) denser refractory aggregates, with apparent density ranging from 2.2 to 2.6 g/cm^3. The value of the characterized chamotte (AD: 1.26 g/cm^3), fall within the lightweight insulating types. This AD is less than that of chamotte (1.428 g/cm^3) presented in Soukup et al., [34] (see Table 3). The chamotte in Soukup et al., [34] was used to process a composite material. It is therefore possible that the apparent density of the studied chamotte is compatible for its use in processing composite roofing tiles.

The major oxide's composition of the analyzed river sand sample shows the predominance of SiO_2 of over the other oxides (Table 4). The SiO_2 content is 65.79 wt.%. This content is followed by that of Al_2O_3 (12.08 wt.%), K_2O (4.1 wt.%), and CaO (1.3 wt.%), respectively. Intermediate and non-negligible contents are that of Na_2O (0.87 wt.%) and Fe_2O_3 (0.57 wt.%). The content of MgO, SO_3, TiO_2, Mn_2O_3, P_2O_5, ZnO, and SrO, are below 0.05 wt.%. The calculated ratios K_2O/ Na_2O, SiO_2 /Al_2O_3, and K_2O/ Al_2O_3 are 5.0, 5.42, and 0.34, respectively. The proportion of LOI is 11.79 wt.%. The 65.79 wt.% is less than the values (76.14-79.37 wt.%) for Maroua river sand samples [27].

Table 4. Major oxides composition for Monatélé-Sanaga river sand and used chamotte.

Sample oxide composition (wt.%)	River Sand	Chamotte
SiO_2	65.79	64.94
Al_2O_3	12.08	12.7
Fe_2O_3	0.57	0.97
CaO	1.3	1.03
MgO	0.04	0.23
Na_2O	0.82	1.27
K_2O	4.1	5.22
SO_3	0.04	0.1
TiO_2	0.02	0.01
Mn_2O_3	0.02	0.03
P_2O_5	-	0.02
ZnO	0.01	0.01
SrO	0.015	0.015
V2O5	-	-
Cr2O3	-	-
ZrO2	-	-
LOI	11.79	12.76
Total	96.53	99.24

LOI = Loss on ignition.

Nafissatou et al., [27] related the silica contents in the Maroua river sand to the presence of quartz. The same suggestion can be done for the studied sand. The Al_2O_3 is much higher than that of Maroua (9.15-9.65 wt.%) which were related to presence aluminosilicate minerals (e.g., feldspars, clay minerals, and micas) [27]. It is probable that the relatively high Al_2O_3 content in the studied sand could lightly be related to presence of aluminosilicate minerals; with their proportion, much higher in the studied sand than in the Maroua river sand. The presence of aluminosilicate minerals is supported by the K_2O/Na_2O and SiO_2 /Al_2O_3 ratios; which are compatible with values for river sand enclosing high K-feldspar and plagioclase; as river sands with high K-feldspar and plagioclase have a K_2O/ $Na_2O > 1$, K_2O/ $Al_2O_3 < 5$, and SiO_2 /$Al_2O_3 > 6$ (cf [27, 36]). For Kagonbé et al., [37], high Al_2O_3 content in sand plays important role during the firing process. This shows that the studied sand is much suitable for the production of tiles or other refractory products. The Fe_2O_3 (0.57 wt.%) is relatively lower than those of Maroua sand samples (1-1.03) which for Nafissatou et al., [27] is a coloring agent for a fired product. The high value of LOI might be due to presence of high content of volatile, hydroxides, organic matters. The studied sand is a high silica-alumina type probably bearing quartz and, aluminosilicate minerals; which might play important role during the firing process leading to the production of roofing tiles.

The major oxide composition for used chamotte sample shows the predominance of SiO_2 of over the other oxides (Table 4). The SiO_2 content is 64.94 wt.%. This content is followed by that of Al_2O_3 (12.7 wt.%), K_2O (5.22 wt.%), Na_2O (1.27 wt.%), CaO (1.03 wt.%), and Fe_2O_3 (0.97 wt.%), respectively. The content of MgO, SO_3, TiO_2, Mn_2O_3, P_2O_5, ZnO, and SrO, are below 0.24 wt.%. The proportion of LOI is 12.76 wt.%. The calculated CaO+ MgO and Na_2O+ K_2O contents are 1.26 wt.% and 6.49 wt.%, respectively. Typical chamotte is geochemically composed of SiO_2 (40 to ≥ 60 wt.%), Al_2O_3 (20 to ≥ 40 wt.%), Fe_2O_3 ≤ 4.0 wt.% (< 2.0 wt.% for high quality material), TiO_2 (< 3.0 wt.%), and CaO+ MgO < 2.0 wt.%, K_2O ≤ 3.0 wt.%, and Na_2O content in trace. Within the quantified oxide values, only that Fe_2O_3, TiO_2, SiO_2, and CaO + MgO fall within the values of typical chamotte. The Al_2O_3 content is less than that of the typical chamotte. The study chamotte can be classified as high SiO_2 and low Al_2O_3 chamotte consequently, low refractoriness; as higher Al_2O_3 in chamotte generally indicates higher refractoriness. The total alkaline (Na_2O+ K_2O: 6.49 wt.%) is more than the value in typical chamotte; classifying the studied chamotte as a relatively high alkaline chamotte. The relatively high SiO_2 and relatively low Al_2O_3, suggests the presence of quartz and aluminosilicate minerals (mullite), as they are frequently found in most chamotte (c.f [38]). Mineralogical studies were not carried to correlate the geochemical data with the mineralogy.

3.2 Characteristics and quality of the processed composite-roofing tiles

The mean values of apparent density (AD) in Table 5, vary from one test specimen to another. In a general point of view, they range from 2.12 to 1.65 g/cm³. Figure 6 generally shows a decrease of AD with the increase in proportion of plastic and that of chamotte. The highest values are those of test specimens in T30F, whereas, the lowest are those in T50F. The mean values of AD vary from 2.12 to 1.65 g/cm³ for 0 %C; from 1.92 to 1.7 g/cm³ for 5 %C; from 1.97 to 1.72 g/cm³ for 10 %C; from 1.84 to 1.64 g/cm³ for 15 %C; from 1.94 to 1.70 g/cm³ for 20 %C; and from 1.90 to 1.64 g/cm³ for 25 %C. The decrease in value of AD with the increase in proportion of chamotte and that of plastic is probably due the fact that sand is much dense than chamotte and plastic.

Table 5. Apparent density for formulated roofing tile's test specimens.

Test specimen with plastic proportion	Mean values of apparent density (g/cm³)					
	0%C	5%C	10%C	15%C	20%C	25%C
T30F	2.12	1.92	1.97	1.84	1.94	1.90
T35F	1.94	1.90	1.97	1.80	1.86	1.80
T40F	1.77	1.84	1.87	1,82	1.64	1.75
T45F	1.75	1.73	1.77	1.79	1.73	1.75
T50F	1.65	1.70	1.72	1.65	1.70	1.64

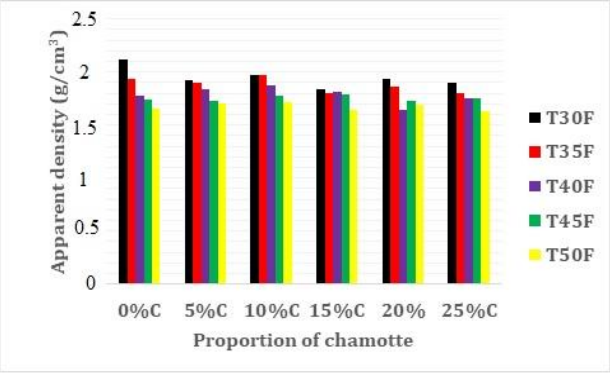

Fig. 6. Line graphs showing the variation of apparent density for processed roofing tiles test specimens.

The apparent density of the used chamotte is 1.26 g/cm³: that of used sand is 1.60 g/cm³. The AD difference between the used chamotte and sand might be the cause of the decrease in density during the partial replacement of sand with chamotte when formulating the test specimens. According the ASTMC373 [39] and ISO10545-3 [40] standards, the AD for roofing tiles ranges from around 2.0 to 2.3 g/cm³ (which shows lower porosity, crucial for freeze-thaw resistance and durability). The values of apparent density for geopolymer roofing tiles studied by Reggiani [9] range from 1.47 to 1.65 g/cm³, and from 1.72 to 1.75 g/cm³. The obtained AD values in this study excepting T30F with 0 %C (2.12 g/cm³), are dominantly less than values required by ASTMC373 [39] and ISO10545-3 [40] standards; but, largely higher than those of geopolymer roofing tiles in Reggiani [9]. This might have positive impact on their resistance.

The mean values of water absorption (Table 6) and plot (Figure 7), show an extreme variation (ranging from 0 to 1.36 %). They range from 0.52 to 0.64 % for 0 % C; from 0.23 to 0.88 for 5 % C; from 0 to 1.17 % for 10 % C; from 0.41 to 1.30 for 15 % C; from 0.23 to 1.36 for 20 % C; and from 0.43 to 0.66 for 25 % C. The highest values are that of formulations T40F with 20 %C, T50F with 15 %C, and T40F with 10 %C, respectively. The lowest values are selectively that of T30F with 5 %C, T30F with 10 %C, T30F with 20 %C, T35F with 10 %C, T40F with 15 %C. The water absorption in T30F and T35F decreases with the increase in proportion of chamotte from 0 to 10 %: increases after 10 % substitution to up to 15 %; but, slight decreases at 20 %C, before, increases at 25 %C. This is not the case for formulations in T40F, T45F, and T50F. An increase in water absorption is noticed when the proportion of chamotte increase from 0 to 10 % for T40F, and from 0 to 5 % for T45F and T50F. According to the AS4046.4 [41] standard, the percentage of water absorption for roofing tiles shall not be more than 10 % for tiles graded for general purpose. According to the ASTMC373 [39] standard, the water absorption for roofing tiles range from < 10 to 15 % or from 6 to 10 %; but, can be less than 3 % for premium tiles; and water absorption more than 10 % indicates lower quality and also lower durability. The water absorption obtained for the formulated roofing tile test specimens dominantly less 1 % (Table 6), are within the range limit (< 3%) for premium roofing tiles as (c.f. [39]); below those of concrete roofing tiles (3.05 to 4.35 %) presented in Sivapriya and Clydin [10], and dominantly less than those of plastic-sand-based composite roofing tiles (0.62-2.25 %) published by Nkotto et al., [11]. If based on the values of water absorption required by the ISO62 [30], ASTMC373 [39], and AS4046.4 [41] standard, and those of tiles presented in Sivapriya and Clydin [10], and Nkotto et al., [11], the processed tiles test specimens are low water absorption types, and more closer to the premium tiles with probably, high quality and high durability, as water absorption more than 10 % indicates lower quality and also lower durability (c.f. [39]).

Table 6. Water absorption mean values for formulated composite roofing tile's test specimens.

Test specimen with plastic proportion	Mean values of water absorption (%)					
	0%C	5%C	10%C	15%C	20%C	25%C
T30F	0.64	0.23	0	0.49	0.23	0.53
T35F	0.65	0.60	0.29	0.69	0.55	0.43
T40F	0.61	0.73	1.17	0.41	1.36	0.66
T45F	0.52	0.88	0.71	0.64	0.49	0.54
T50F	0.52	0.88	0.66	1.30	0.51	0.63

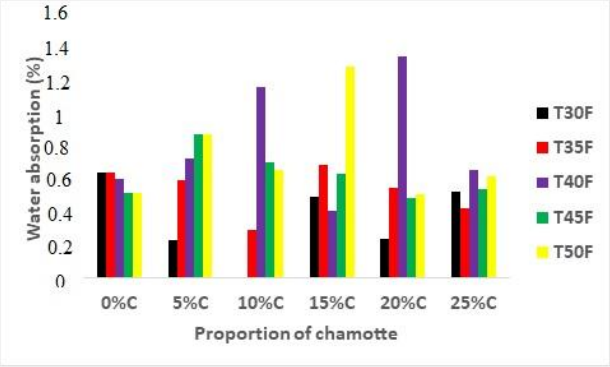

Fig. 7. Line graph showing the variation of water absorption for processed roofing tiles test specimens.

The mean values of porosity vary from 0 to 2.03 % (Table 7). They also show an extreme variation (Figure 8). They vary from 0.88 to 1.19 % for 0 %C, from 0.41 to 1.61 % for 5 %C, from 0 to 1.87 % for 10 %C, from 0.69 to 1.99 % for 15 %C, from 0.41 to 2.03 % for 20 %C, and from 0.79 to 1.08 % for 25 %C. The main picks of porosity are that of formations T40F with 20 %C, T50F with 15%C, T40F with 10 %C and T45F with 5 %C; whereas, the lowest values are selectively that of T30F with 5 %C, T30F with 10 %C, T30F with 20 %C, T35F with 10 %C, T40F with 15 %C. This was almost the same case with water absorption. It therefore shows a correlation between the water absorption and porosity. In general point of view, the values of porosity show a slight increase from T30F to T35F and slight decrease to up to T50F. For 5 %C, an increase in porosity is noticed from T30F to T45F. For

10%C, an increase in porosity is noticed from T30F to T40F, and a decrease, after T40F. This is the same for 20 %C. For 15 %C, an. increase is observed from T30F to T35F, and from T40F to T50F. The partial replacement of sand with chamotte and the increase in proportion of plastic in the different formulations selectively reduce the proportion porosity. According to the ASTMC373 [39] standard, the values of porosity for roofing tiles roughly range from 14 to 20 %. The values of porosity for plastic-sand-based composite roofing tiles published by Nkotto et al., [11] vary from 1.26-4.37 %. The obtained mean values of porosity are less those required by ASTMC373 [39] standard, and dominantly less than those of plastic-sand-based composite roofing tiles in Nkotto et al., [11]; which classify the formulated test specimens as less porous types.

Table 7. Porosity mean values for formulated composite roofing tile's test specimens.

Test specimen with plastic proportion	Mean values of porosity (%)					
	0%C	5%C	10%C	15%C	20%C	25%C
T30F	1.16	0.41	0	0.85	0.41	0.91
T35F	1.19	1.07	0.62	1.16	1.00	0.79
T40F	1.04	1.27	1.87	0.69	2.03	1.05
T45F	0.91	1.61	1.27	1.17	0.94	0.92
T50F	0.88	1.41	1.08	1.99	0.93	1.08

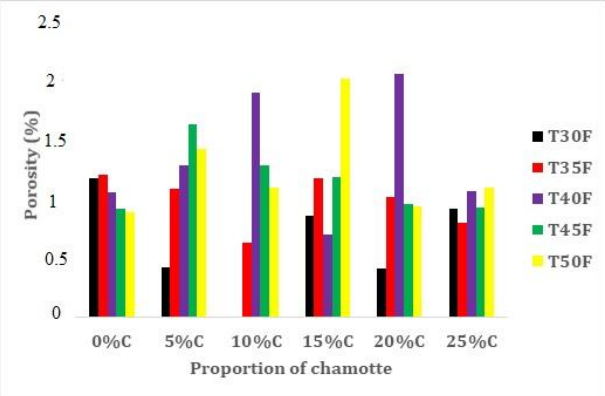

Fig. 8. Line graph showing the variation of porosity for processed roofing tiles test specimens.

The flexural strength (FS) results in Table 8 and plot in Figure 9, show heterogeneity; both for the increase in proportion of plastic and that of chamotte. For 0 %C test specimens, the flexural strength varies from 3.68 to 1.86 MPa from T30F to T50F (which shows a decrease of strength with the increase in proportion plastic). It varies from 3.98 to 1.53 MPa when 5 %C is used. The same strength value (3.67 MPa) is obtained for T30F (0 %C), T30F (5 %C), T35F (5 %C), T45F (5 %C), and T40F (10 %C). A decrease of strength is recorded after T40F. The strength values vary from 1.22 to 4.29 MPa with a decrease of strength from T30F to T50F (when 10 %C is used). Which is similar to the behavior when 0% C is used, but different, when 5 %C is used. For 15 % C replacing sand, the flexural strength varies from 1.53 to 5.24 MPa, with the value 3.37 MPa for T45F (20 %C) being similar to that of T45F (15 %C). A drecrease of strength is observed from T30F to T40F and after T45F. The flexural strength for specimens formulated with 20 %C partial replacement of sand ranges from 1.84 to 4.59 MPa; with the same strength (3.98 MPa) obtained for T35F (20 %C) and T40F (20 %C).

Table 8. Flexural strength mean values for formulated composite roofing tile's test specimens.

Test specimen with plastic proportion	Mean values of flexural strength (MPa)					
	0%C	5%C	10%C	15%C	20%C	25%C
T30F	3.67	3.67	4.29	5.20	4.59	6.12
T35F	3.06	3.67	3.98	3.06	3.98	4.59
T40F	3.06	3.98	3.67	2.45	3.98	2.45
T45F	2.76	3.67	3.37	3.37	4.29	4.59
T50F	1.84	1.53	1.22	1.53	1.84	2.45

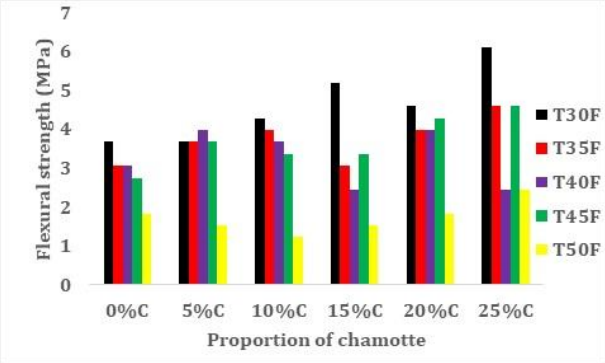

Fig.9. Line graph showing the variation of flexural strength for processed composite roofing tiles test specimens.

This value is similar to that of T35F (10 %C) and T40F (5 %C). For formulations with 25 %C; the FS values vary from 2.45 to 6.12 MPa; with the same strength (4.59 MPa) obtained for T35F (25%C) and T45F(25%C). The lowest value 2.45 MPa is found in both T50F (25 %C) and T40F (25 %C). The highest FS values are generally those of formulations T30F, and that of 25 %C. The lowest values are those of T50F. It is not easy to correlate the low FS of T50F to high porosity and high-water absorption, since the values of porosity and water (Table 8) are variable (relatively high for some specimens and lower for others). The obtained FS compares to those of roofing tiles published by other authors and the standardized values show some similarities and differences. The FS values for plastic-sand composite roofing tiles test specimens published by Nkotto et al., [11], vary from 0.23 to 5.32 MPa. Those of concrete tiles by Varela et al., [6], vary from 0.24 to 0.51 MPa. The standardized FS values for concrete roofing tiles vary from 0.24 to 0.89 MPa, or higher depending on additives/materials [6]. The obtained FS values (1.22 -6.12 MPa with most values exceeding 3.3 MPa) are generally more than those of specimens published in Nkotto et al., [11]. They are largely more than standard values for concrete roofing tiles and those of specimens published by Varela et al., [6]. The FS values for the test specimens make them relatively much resistant.

Table 9. compression strength mean values for formulated composite roofing tile's test specimens.

Test specimen with plastic proportion	Mean values of compression strength (MPa)					
	0%C	5%C	10%C	15%C	20%C	25%C
T30F	14.29	19.84	15.51	19.59	13.88	16.33
T35F	17.14	18.37	14.69	13.71	14.69	17.96
T40F	14.69	14.69	15.84	13.88	13.88	10.61
T45F	9.80	12.49	15.59	18.78	14.69	13.88
T50F	11.84	14.69	15.92	15.92	15.10	13.06

The mean values of compression strength (CS) and plotted data show a variation from one test specimen to another (see Table 9 and Figure 10). They range from 9.80 to 17.14 MPa for 0 %C partial replacement, and from 12.49 to 19.84 MPa for 5 %C replacement (with the values been generally higher than those of 0 %C replacement); showing that, the increase of 5 % chamotte have increased the CS. For 10 % chamotte replacement (10 %C), the CS varies from 14.69 to 15.92 MPa, with an increase of CS for T40F, T45F and T50F. For 15 %C, the CS varies from 13.71 to 19.59 MPa (with an increase of strength for T30F, T45F, and T50F). For 20 %C partial replacement, the CS ranges from 13.88 to 15.10 MPa; with two specimens T30F and T40F having the same CS (13.88 MPa), similar to that of T40F (15 %C). The CS (14.69 MPa) of T35F (20 %C) is similar to that of T45F (20 %C), T35F(10 %C); T40F (0 %C), T40F(5 %C), and T50F (5%C). For 25%C replacement, the CS varies from 10.61 to 17.67 MPa with 13.88 being the same as for T30F (20%C), T40F (20%C), and T40F (15 %C). The obtained CS, compared with those of roofing tiles published by other authors and standardized values, show some similarities and differences. The CS values for sand-plastic composite roofing tile's test specimens published by Nkotto et al., [11], vary from 4.67 to 7.13 MPa. Those of concrete roofing tiles published by Varela et al., [6], vary from 0.1 to 0.39 MPa. Those published by Rajalakshmi et al., [2] for agro-industrial roofing tile and ordinary clay roofing tile, vary from 1.30 to 8.21 MPa. The standard range of CS of clay roofing tiles varies from 8 to 10 MPa [2]. The CS values (9.76-19.84 MPa) for the studied test specimens are dominantly higher than the standard CS for ordinary clay roofing tiles, and are largely more than those of roofing tiles test specimens published in Nkotto et al., [11], Varela et al., [6], and Rajalakshmi et al., [2]. This indicates that the processed specimens exhibit higher mechanical strength much than the compared tiles.

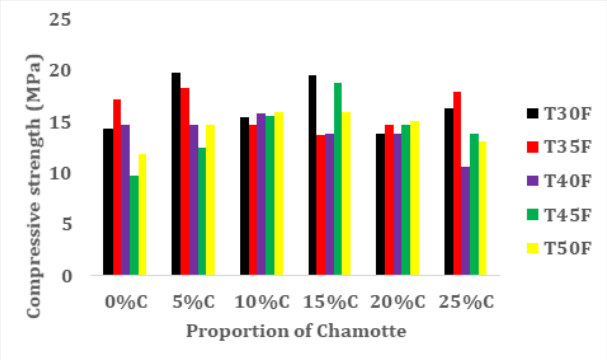

Fig. 10. Line graph showing the variation of compression strength for processed composite roofing tiles test specimens.

The use of sand, chamotte, and plastic to process composite roofing tile increases the flexural strength, compression strength and produces high resistant tiles. This could be attributed the binding effect of molten plastic and the relatively high Al_2O_3 content in both chamotte and the river sand. For Kagonbé et al., [37], high Al_2O_3 content in sand plays important role during the firing process. After the compression strength, flexural strength, porosity, water absorption, and apparent density test results carried out on formulated specimens, composite roofing tiles were processed with this formulation (30 % of plastic+ 10 % of chamotte + 50 % river sand) (see prototype in Figure 11). This high resistance polymer-composite roofing tiles, processed by incorporating recycled PET plastic waste and local aggregates (river sand and chamotte) represents a promising route toward sustainable construction material with reduced environmental footprint.

Fig. 11. Processed river sand-chamotte-¨PET plastic-based composite roofing tile prototype with 30 % of PETplastic+10 % of chamotte+ 60 % of sand.

4. CONCLUSION

Based on the work characterizing Monatélé-Sanaga river sand and chamotte, and combining them with PET plastic in a thermal processing of sand-chamotte-plastic composite roofing tiles and results obtained, the following conclusions were made:

1. The grain size distribution parameters (fineness modulus, uniformity coefficient, and curvature coefficient), and specific gravity for Monatélé Sanaga river sand show that it is medium to a bit coarse-grained, well graded and good for concrete production. The apparent density classifies it as not well sorted and slightly low-density sand. Geochemical feature of the studied sand shows a relatively high SiO_2 with significant Al_2O_3 suggesting the presence of quartz and aluminosilicates minerals important for the production roofing tiles.

2. Particle size analysis and specific gravity test carried out on crushed chamotte classifies it as fine to coarse-grained and very low-SG type; good for composite roofing tiles processing. The apparent density of the chamotte classifies it as lightweight insulating type (compatible with those used in processing composite roofing tiles). The geochemical feature classifies it as high SiO_2-low Al_2O_3 and slightly high alkaline chamotte suggesting the presence of quartz and aluminosilicate minerals (interesting in tiles processing).

3. Quality (apparent density, water absorptions, porosity, flexural and compression strength) tests carried out formulated test specimens show a variation. The apparent density decreases with the increase in proportion of chamotte and plastic, probably due the fact that sand is much dense than chamotte and plastic. The water absorption places the formulated test specimens within the low water absorption type, closer to the premium tiles. The porosity classifies the test specimens within the less porous types. The flexural and compression strength more than standard values for concrete roofing tiles and ordinary clay-based roofing tiles, shows that the processed test specimens are much resistant.

Acknowledgements

The authors would like to thank the Local Materials Promotion Authority (MIPROMALO) for providing chamotte sample and laboratory facilities for grain size distribution analysis, physical and mechanical tests. They also extend their gratitude to CIMENCAN Figuil for providing laboratory facilities for geochemical analysis of sand and chamotte samples.

REFERENCES

[1] C. Jayasinghe, M. H. P. J. De Silva, D. M. M. P. Dissanayake, and C. T. K. I. Fernando, "Engineering properties of micro concrete roofing tiles," *Engineer Journal of the Institution of Engineers Sri Lanka*, vol. 39, no. 3, p. 35, Jul. 2006, doi: 10.4038/engineer.v39i3.7191.

[2] R. S. Rajalakshmi, "Comparing the Strength Behavior of Agro-Industrial Roofing Tile with Ordinary Clay Roofing Tile," *International Journal of Engineering Research And*, vol. V9, no. 05, May 2020, doi: 10.17577/ijertv9is050284.

[3] A. A. Akinwande, A. A. Adediran, O. A. Balogun, Y. V. Adetula, T. M. A. Olayanju, and O. O. Agboola, "Material Selection for the Production of Roof Tiles using Digital Logic Method," IOP Conference Series Materials Science and Engineering, vol. 1107, no. 1, p. 012022, Apr. 2021, doi: 10.1088/1757-899x/1107/1/012022.

[4] B. S. Aravind and G. P. U. Vinyas, "An experimental study on cement and fibre based roofing tile as an alternative to Mangaluru tile," *Int. Res. J. Eng. Technol.,* vol. 7, iss.6, pp. 3908-3912, 2020.

[5] Y. Liu, W. M. Yang, and M. F. Hao, "Research on mechanical performance of roof tiles made of tire powder and waste plastic," *Advanced Materials Research*, vol. 87–88, pp. 329–332, Dec. 2009, doi: 10.4028/www.scientific.net/amr.87-88.329.

[6] B. D. Varela, J. L. S. Quito, and N. C. Piaza, "Flexural and Compressive Strength of Concrete Tiles with Different Levels of Partial Substitution of Pulverized Solid Waste Materials for Gravel," *OALib*, vol. 02, no. 01, pp. 1–10, Jan. 2015, doi: 10.4236/oalib.1101187.

[7] J. W. On *et al.*, "Mechanical and Physical Properties of Roof Tile Prepared from Sugar Cane Fiber," *The International Journal of Advanced Culture Technology*, vol. 3, no. 1, pp. 86–89, Jun. 2015, doi: 10.17703/ijact.2015.3.1.86.

[8] A. K. FiGen, Ü. Özçay, and S. PiŞkiN, "Manufacturing and characterization of roof tiles a mixture of tile waste and coal fly ash," *Süleyman Demirel Üniversitesi Fen Bilimleri Enstitüsü Dergisi*, vol. 21, no. 1, p. 224, Jan. 2017, doi: 10.19113/sdufbed.33169.

[9] A. Reggiani, "Geopolymer roof tile," in *Ceramic engineering and science proceedings*, 2019, pp. 225–232. doi: 10.1002/9781119543381.ch20.

[10] S. Sekhar, A. Thomas, and P. A. Clydin, "Strength characteristics of geopolymer concrete floor tiles on various mix proportions," *Open MIND*, vol. 10, no. 6, Jun. 2021, doi: 10.5281/zenodo.18607233.

[11] L. I. N. Nkotto, L. J. Ntamag, V. C. N. Nzouakoi, J. S. Kanda, M.-A. J. F. Manjeh, and J. V. S. Metekong, "Formulation and characterization of a tile based on plastic waste and alluvial sand Sanaga-Cameroon," *American Journal of Innovative Research and Applied Sciences*, vol. 16, no. 2, pp. 42–53, 2023.

[12] D. R. S. D. Santos, O. J. C. Fernandez, D. M. Porfírio, M. F. R. De Lima, R. S. D. Santos, and P. M. P. Silva, "Technological characterization of clay and chamotte incorporated in handmade ceramics," *Materials Research*, vol. 28, no. suppl 1, Jan. 2025, doi: 10.1590/1980-5373-mr-2025-0095.

[13] A. F. Zoum et al., "Physico-mechanical characterization of micro-concrete roofing tiles produced from Bambui (North West Cameroon) and Garoua I (North Cameroon) river sands," *J. Mater. Environ. Sci.,* vol. 15, iss. 4, pp. 552-563, 2024.

[14] C. V. Amaechi *et al.*, "An overview of composites as construction materials for the Development of sustainable structures," *Materials Today Sustainability*, vol. 33, p. 101298, Jan. 2026, doi: 10.1016/j.mtsust.2025.101298.

[15] S. Prakas, "Impact of plastic pollution on environment and human health: an overview," *IRE Journals*, vol. 1, no. 5, pp. 53-59, 2017.

[16] S. Aluvihara, C. S. Kalpage, and B. S. Chauhan, "Characterizations of some selected clay types for cost effective wastewater treatments," *Journal of Materials and Engineering*, vol. 3, no. 4, pp. 417–429, Jan. 2025, doi: 10.61552/jme.2025.04.006.

[17] E. K. Orhorhoro, "A review of plastic waste management for a sustainable environment: Composition and approaches," *European Journal of Sustainable Development Research*, vol. 9, no. 3, p. em0314, May 2025, doi: 10.29333/ejosdr/16359.

[18] R. U. Halden, "Plastics and Health Risks," *Annu. Rev. Public Health*, vol. 31, no. 1, pp. 179–194, Mar. 2010, doi: 10.1146/annurev.publhealth.012809.103714.

[19] Association Française de Normalisation (AFNOR), *NF P 94-057: Sols: reconnaissance et essais—Analyse granulométrique des sols—Méthode par sédimentation*. Paris, France: AFNOR, 1992.

[20] European Committee for Standardization (CEN), *EN 12620:2013, Aggregates for Concrete*. Brussels, Belgium: CEN, 2013.

[21] European Committee for Standardization (CEN), *EN 1097-6:2013, Tests for Mechanical and Physical Properties of Aggregates—Part 6: Determination of Particle Density and Water Absorption*. Brussels, Belgium: CEN, 2013.

[22] ASTM International, *ASTM D2854, Standard Test Method for Apparent Density of Activated Carbon*. West Conshohocken, PA, USA: ASTM International, 2024.

[23] T. Hamadou, N. S. Kanouo, J. Dikwa, A. B. Tchamba, and L. L. Duna, "Cement kiln dust in CIMENCAM Figuil (North Cameroon): characteristics and recycling as additives for blended cement production," *SN Applied Sciences*, vol. 5, no. 7, Jun. 2023, doi: 10.1007/s42452-023-05401-z.

[24] ASTM International, *ASTM C20-00, Standard Test Methods for Apparent Density, Porosity, Water Absorption, Specific Gravity, and Bulk Density of Burned Refractory Brick and Shapes by Boiling Water*. West Conshohocken, PA, USA: ASTM International, 2000.

[25] Association Française de Normalisation (AFNOR), *NF P18-459, Béton – Essai pour béton durci – Essai de porosité et de masse volumique*. Paris, France: AFNOR, 2010.

[26] European Committee for Standardization (CEN), *EN 12390-2:2019, Testing Hardened Concrete—Part 2: Making and Curing Specimens for Strength Tests*. Brussels, Belgium: CEN, 2019.

[27] M. Nafissatou *et al.*, "Potential use of the Maroua (Far North, Cameroon) river sand as construction materials and degreasing agent for earthenware ceramics," *Discover Applied Sciences*, vol. 7, no. 2, Jan. 2025, doi: 10.1007/s42452-024-06255-9.

[28] F. Ghomari and A. Bendi-Ouis, *Sciences des matériaux de construction*. Tlemcen, Algeria: Department of Civil Engineering, Abou Bekr Belkaid University, 2008.

[29] ASTM International, *ASTM C33/C33M-16, Standard Specification for Concrete Aggregates*. West Conshohocken, PA, USA: ASTM International, 2016.

[30] International Organization for Standardization, *ISO 62:2008, Plastics—Determination of Water Absorption*. Geneva, Switzerland: ISO, 2008.

[31] H. E. Opara, U. G. Eziefula, and B. I. Eziefula, "Comparison of physical and mechanical properties of river sand concrete with quarry dust concrete," *Selected Scientific Papers*, vol. 13, no. s1, pp. 127–134, Mar. 2018, doi: 10.1515/sspjce-2018-0012.

[32] M. W. M. Abdias, M. M. Blanche, U. J. P. Nana, H. F. Abanda, N. François, and P. Chrispin, "River Sand characterization for its use in Concrete: a revue," *Open Journal of Civil Engineering*, vol. 13, no. 02, pp. 353–366, Jan. 2023, doi: 10.4236/ojce.2023.132027.

[33] M. Al-Taie and H. S. Z. Abu-Hamatteh, "Influence of the grain size distribution of chamotte on the properties of fire-clay refractory bricks,". *Sixth International Conference on the Geology of Arab World (JAW 6) Cairo-Egypt, 11th -14th Feb. 2002, Editor: El-Syed, A. A. Yousef, Faculty of Science, Cairo University*, vol. 02, pp 839- 844, 2002.

[34] A. Soukup, M. Vakili, and P. Hájková, "Effect of waste metal and chamotte fillers on the thermal and mechanical properties of geopolymer composites for energy storage applications," *Materials*, vol. 18, no. 16, p. 3853, Aug. 2025, doi: 10.3390/ma18163853.

[35] Association Française de Normalisation (AFNOR), *NF P18-554, Granulats—Mesures des masses volumiques, de la porosité, du coefficient d'absorption et de la teneur en eau des gravillons et cailloux*. Paris, France: AFNOR, 1979.

[36] F. O. Amiewalan and F. A. Lucas, "Geochemical characterization of FE-1 well, Onshore Western Niger Delta Basin, Nigeria," *Journal of Applied Science and Environmental Management*, vol. 24, no. 2, pp. 381–391, Apr. 2020, doi: 10.4314/jasem.v24i2.26.

[37] B. P. Kagonbé, D. Tsozué, A. N. Nzeukou, and S. Ngos, "Mineralogical, physico-chemical and ceramic properties of clay materials from Sekandé and Gashiga (North, Cameroon) and their suitability in earthenware production," *Heliyon*, vol. 7, no. 7, p. e07608, Jul. 2021, doi: 10.1016/j.heliyon.2021.e07608.

[38] L. Díaz-Tato, J. F. López-Perales, Y. González-Carranza, J. E. C. De León, and E. A. Rodríguez-Castellanos, "Physico-Mechanical properties of an aluminosilicate refractory castable obtained after chamotte waste recycling by firing method," *Waste*, vol. 3, no. 4, p. 35, Oct. 2025, doi: 10.3390/waste3040035.

[39] ASTM International, *ASTM C373-17, Standard Test Methods for Determination of Water Absorption and Associated Properties by Vacuum Method for Pressed Ceramic Tiles and Glass Tiles and Boil Method for Extruded Ceramic Tiles and Non-Tile Fired Ceramic Whiteware Products*. West Conshohocken, PA, USA: ASTM International, 2017.

[40] International Organization for Standardization, *ISO 10545-3:2018, Ceramic Tiles—Part 3: Determination of Water Absorption, Apparent Porosity, Apparent Relative Density and Bulk Density*. Geneva, Switzerland: ISO, 2018.

[41] Standards Australia, *AS 4046.4-2002, Roofing Tiles—Methods of Testing, Part 4: Determination of Water Absorption*. Sydney, NSW, Australia: Standards Australia, 2002.